



## **Analysis of multispectral RPA images for vegetation mapping in riparian areas**

**Adão Robson Elias**

PhD Professor, UTFPR, Brazil.  
robsonelias@utfpr.edu.br

**Edson Luís Piroli**

PhD Professor, UTFPR, Brazil.  
Edson.piroli@unesp.br

**Henrique dos Santos Felipetto**

PhD Professor, UTFPR, Brazil.  
felipetto@utfpr.edu.br

#### ABSTRACT

Riparian vegetation is important in ecological maintenance along river banks. Vegetation Indices (VIs) and Leaf Area Index (LAI) are indices that can be indirectly correlated with plant development and health. Therefore, this study aimed to test the effectiveness of using Remotely Piloted Aircraft (RPA) in acquiring multispectral images for creating VIs and indirectly obtaining LAI. Orthoimages were obtained of 3 sample areas along the Pardo River Hydrographic Basin (PRHB), which comprises 3 classes of vegetation, the forest at the source of the Pardo River, a grassland vegetation area and a forest area. The sampling areas were cut into 9 plots of 9 x 9 m and distributed across the orthoimages. An RPA of DJI's Phantom 4 Multispectral model was used to obtain multispectral images. From the orthoimages, VIs were generated, such as NDVI (Normalized Difference Vegetation Index) and SAVI (Soil Adjusted Vegetation Index), then the corresponding LAI was generated. The results show that simple linear correlation analyzes identified LAI as a regression-dependent variable, demonstrating a high significance with the independent variables NDVI and SAVI. It was possible to verify that the vegetation classes and their structural heterogeneities influenced the adjustments of the LAIs. It is concluded that the images obtained by multispectral RPA presented very high spectral, spatial and temporal resolution, being suitable for the management and constant monitoring of permanent preservation areas (PPA).

**KEYWORDS:** Drone, NDVI, Leaf Area Index, Rio Pardo River.

## 1 INTRODUCTION

Over the years, there has been an increase in attention to PPA areas, to which many environmental monitoring, protection and management projects have been directed. In this context, photogrammetry and Remote Sensing (RS) techniques are being used to monitor areas of environmental interest and agricultural production in recent decades. Recently, images obtained by drones or Remotely Piloted Aircrafts (RPAs) have been significantly integrated into research related to these themes (FELIPETTO et al., 2023).

Monitoring riparian areas through vegetation mapping, providing information about their distribution, quantity and quality of the various plant species present in a given area, has become one of the main focuses of river basin management (PIROLI, 2022). However, it is only recently that solutions based on high spatial, temporal and spectral resolution technology have begun to be implemented in operational monitoring to overcome the typical problems of surveying wetlands and difficult-to-access areas, such as high cost, time consumption and low accessibility (FUSTINONI, 2021). RS using RPA is an ally that can quickly provide qualitative and quantitative information on the imaged feature, and is a technology widely used for monitoring vegetated areas, which allows various types of assessments, such as plant growth and health status (ELIAS, 2019). Furthermore, it can be integrated with the Geographic Information System (GIS) to refine the analysis from a spatial and temporal point of view. RS and GIS make it possible to carry out assessments of wetlands in various scenarios, studying in detail changes in vegetation in space and time. Therefore, they are effective tools for decision-making and for designing monitoring programs (ADAM et. al, 2010).

According to Husson (2017), Unmanned Aerial Vehicles (UAVs) bring advantages such as obtaining images with centimeter resolution. Thus, they make UAV-based photogrammetry and RS tools fundamental for mapping and monitoring terrestrial and aquatic ecosystems, such as PPAs at a fine scale, even allowing the structural recognition of individual plant species.

With the use of RPAs in RS, many image processing practices could be implemented for the quantification and qualification of an immense range of vegetation biophysical parameters, such as Leaf Area Index (LAI), biomass and its productivity, percentage of soil cover, photosynthetic activity and the characterization and monitoring of vegetation areas (LIMA et al, 2017). According to Ferraz et al. (2013), in principle, these estimates are made using the so-called Vegetation Indices (VIs) and other variables extracted from RS images, presenting the great advantage of providing not only accessibility of information in remote and difficult-to-access locations, but also savings, in terms of field work, when compared to traditional methods.

One of the most used VIs for monitoring soil cover is the Normalized Difference Vegetation Index (NDVI) (ROUSE et al., 1973). NDVI is widely used to carry out LAI (ALMEIDA et al., 2015) and aerial biomass (FERRAZ et al., 2013) calculations.

Seeking to minimize the action of soil reflectance on NDVI, Huete (1988) incorporated the L factor into the NDVI equation, giving rise to the Soil-Adjusted Vegetation Index (SAVI). The L factor promotes an adjustment according to the soil cover, seeking to minimize the effects of its color on the index results. According to the characteristics of the soil and the type of cover, the L factor can vary between 0 (dense vegetation) and 1 (sparse vegetation) (WASHINGTON-ALLEN et al., 2004). The L value equal to 0.5 has been used in most cases, regardless of the type of soil and intermediate density vegetation cover. In denser areas, the constant  $L = 0.25$  is adopted. When L is equal to 0, SAVI is equal to NDVI (HUETE, 1988; MENESES and ALMEIDA, 2012).

Other factors can influence VIs. According to Zhang et al. (2014) leaf pigments, mainly chlorophyll and carotenoids, are important compounds for photosynthesis, dissipation of light radiation and other biological functions. Therefore, variation in the amount of these pigments may be indicative of changes in plant development, senescence or stress.

According to Galvíncio et al. (2020), the Leaf Area Index (LAI) can be considered an environmental variable influenced by climate, which reflects the seasonality of vegetation, and it is one of the necessary parameters for understanding the physiological processes of plants.

Therefore, one of the challenges and hypotheses of this research is to demonstrate that by obtaining multispectral photogrammetric images from RPAs it is possible to generate Vegetation Indices (VI) capable of generating essential information for the conservation management of riparian vegetation areas. Furthermore, from the vegetation indices it is possible to obtain Leaf Area Indices (LAI) that can demonstrate the biomass situation of these vegetations.

Due to environmental issues and sensitivity to climate change and the effects of land use, permanent preservation areas are under environmental protection, requiring regular monitoring and effective management actions, where RPAs can be great allies in these interactions (FUSTINONI, 2021).

## 2 OBJECTIVE

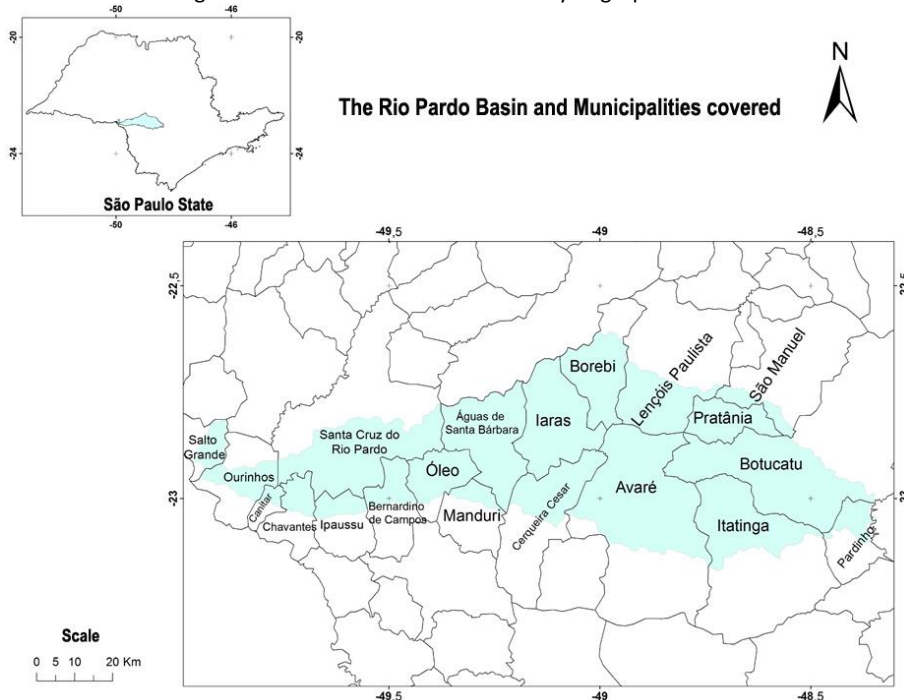
This research aimed to analyze the vegetation conditions of some riparian areas of the Pardo River Hydrographic Basin (PRHB), based on aerial images obtained by RPA, in order to test the effectiveness of using this platform in the acquisition of multispectral orthoimages, as well as how to prepare VIs and indirectly obtain the LAI. The results should serve as input for the planning, handling and environmental management of PRHB and others that present similar conditions.

### 3 METODOLOGY

Surveys of the sample areas were carried out along the Pardo River Hydrographic Basin (PRHB), which is located in the central-southern portion of the State of São Paulo and covers areas of 20 municipalities as shown in Figure 1.

In this research, a DJI P4 Multispectral drone model (Figure 2) with a rotating wing (has propellers like helicopters – vertical takeoff and landing) was used, being the aircraft most suitable for the proposed project, as it does not require space for launch and landing (ELIAS, 2019). The P4 Multispectral is equipped with six imaging bands such as integrated RGB, blue (450 nm wavelength), green (560 nm), red (650 nm), Red edge (RE) (730 nm) and Near-infrared (NIR) (840nm). Figure 3 shows the P4 Multispectral camera. The weight of the aircraft is 1,487 g, with a maximum flight autonomy of approximately 27 min, maximum speed of 14 m/s, with a 3-axis gimbal. The aircraft's positioning is obtained from an external GNSS sensor, capable of capturing signals from NAVISTAR-GPS, GLONASS, Galileo and Beidou.

Figure 1 - Location of the Pardo River Hydrographic Basin.



Source: The authors, 2023.

Figure 2 - DJI P4 Multispectral drone model.



Source: <https://www.dji.com/br/p4-multispectral>.

For the surveys, it was necessary to carry out flight plans for the sampling areas separately. The dimensions of the imaged areas were planned taking into account not only the platform's maximum autonomy, but also a safety margin for in-flight emergencies, which was approximately 12 minutes of total survey time.

Figure 3 - Multispectral camera.



Source: <https://www.dji.com/br/p4-multispectral>.



Flight time could also change, even at the time of carrying out the survey, as the higher the wind speed, the greater the battery consumption and the shorter the flight range. Wind, rain and other adverse weather conditions can even cause the aircraft to crash in an extreme situation. Therefore, the field activity was planned and carried out on days when the weather conditions were suitable. The flights were carried out between 10 am and 2 pm, in order to minimize shadows on the vegetation. The flight plan configurations were: Flight height 51 m, side strip with coverage of 55% and frontal with 60%, Flight speed of 33 km/h and Ground Sample Distance (GSD) of 2.7 cm/pix.

The GSD is a fundamental calculation in flight planning, as it presents the resolution of the aerial photo on the ground (MIKHAIL, 2001), the GSD can be defined by Equation 1 below:

$$GSD = \frac{h \cdot s}{f} \quad (\text{Equation 1})$$

Where h is the flight height, s is the pixel size and f is the focal length.

The flight plans were created using the DJI GS Pro, which is DJI's official program for surveys with the P4 multispectral. The GS Pro features a pre-programmed flight line plan, with a graphical flight path plan overlaid on a Google Maps image base ([www.dji.com](http://www.dji.com)).

Three areas were selected along the basin with different vegetation classes, but all belonging to the Pardo River permanent preservation area (PPA), with the survey carried out from upstream to downstream, as described below:

Source (area = 1 ha) with secondary tree vegetation;

Forest (area = 0.78 ha) with riparian vegetation;

Grassland (area = 0.36 ha) with field vegetation.

Orthomosaics were processed using Agisoft Metashape Professional 1.6.5 build 11249 (64 bits) 3D reconstruction from multiple views ([www.agisoft.com](http://www.agisoft.com)). Obtaining vegetation indices and data analysis were carried out using QGIS 3.16 ([www.qgis.org](http://www.qgis.org)). The reference system adopted was SIRGAS 2000, UTM Zone 22 S, central spindle -51 W.

The aerial images were selected and cropped into areas of interest (Sample). Also, procedures were carried out to generate colored composition (RGB) for better visualization and spatial location of the different features of interest (individuals and vegetation species). Subsequently, the RGB images, from the red and near infrared bands, were processed to create the Vegetation Indices (VI) NDVI (ROUSE et al., 1973), SAVI (HUETE, 1988) and LAI (ALLEN, 2002), presented by Equations 2, 3 and 4 respectively. Still in QGIS, shapefiles were created for the sample polygons of the plots (9 x 9 meters), where the images of the vegetation indices were cut using the shapefiles and determining the average values of these indices for each plot, and these values were used in the regressions linear. The statistical procedures referring to the shapefiles of the sample polygons of the plots were carried out using the QGIS statistical tool.

$$NDVI = \frac{(NIR - RED)}{(NIR + RED)} \quad (\text{Equation 2})$$

Where NIR is the near infrared band and RED is the red edge.

$$SAVI = \frac{(1+L) \times (NIR - RED)}{(L + NIR + RED)} \quad (\text{Equation 3})$$

Where L is constant referring to the degree of soil coverage and can vary from 0 to 1

$$LAI = \frac{\ln\left(\frac{0.69 - SAVI}{0.59}\right)}{0.91} \quad (\text{Equation 4})$$

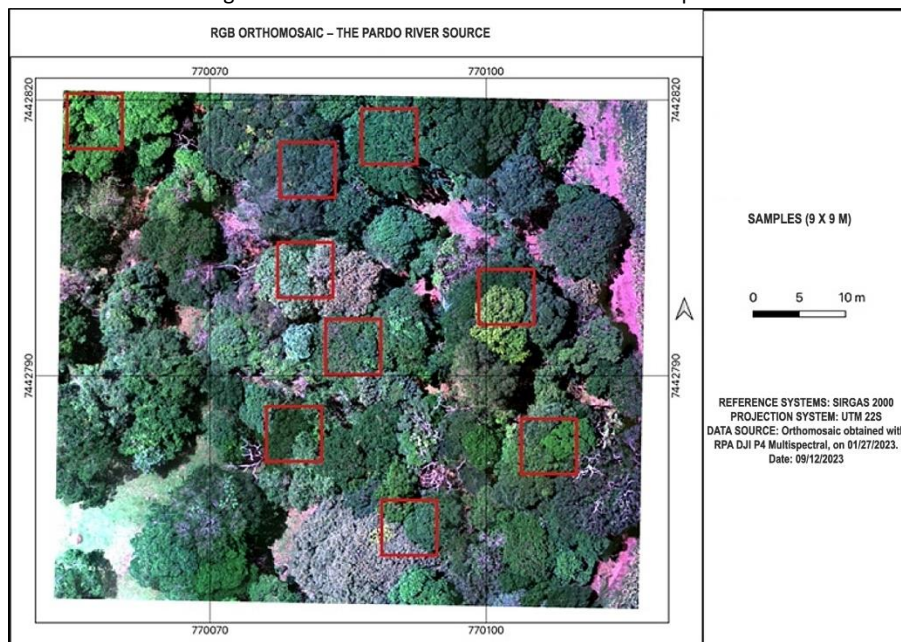
Where SAVI is the Soil-Adjusted Vegetation Index.

The relationships between the dependent variables LAI and the independent variables NDVI and SAVI, which were calculated based on the image samples obtained in this study, were subjected to normal distribution tests of the statistical model. To this end, the F test and t – Student test were applied at a significance level of 5% probability and subsequently applied to determine the result of the regression models (FONSECA, 2009). Regression analysis was carried out using the simple linear regression modeling method, where all calculations were carried out in Microsoft Excel (License from the author). The RGB orthomosaics were produced with the sample polygons of the 9 x 9 meter plots and the NDVI, SAVI and LAI maps for all vegetation classes studied.

#### 4 RESULTS AND DISCUSSION

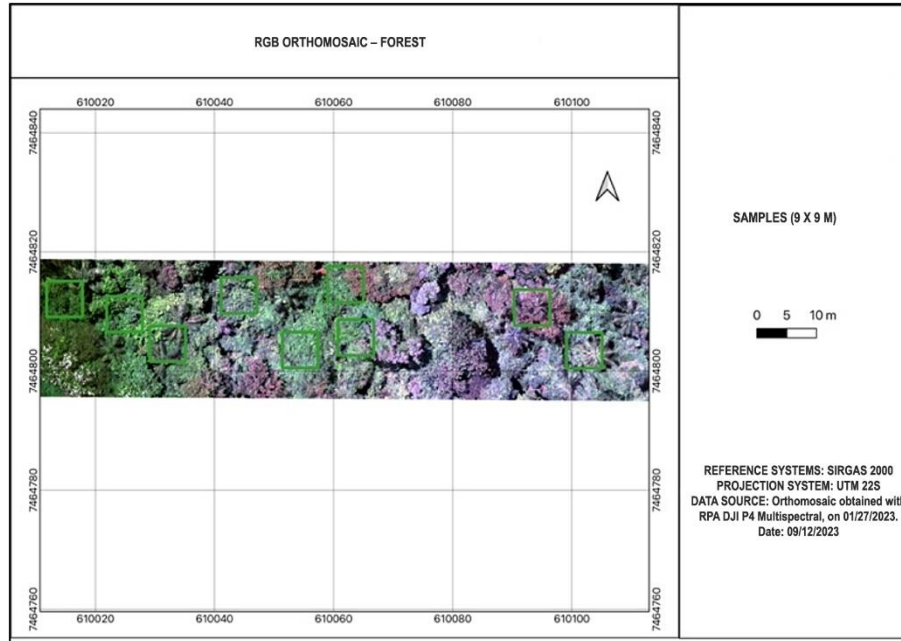
In the RGB orthomosaics (bands 3, 2 and 1) obtained by aerophotogrammetric processing, it is possible to observe the vegetation classes called Source (Figure 4), Forest (Figure 5) and Grassland (Figure 6) with high spatial resolution, making it possible to enlarge the images digitally to the point of identifying individuals and in some cases, plant species (BOOM et al., 2006; ZWEIG et al., 2015; HUSSON et al., 2017; ELIAS, 2019).

Figure 4 - Orthomosaic in RGB of the Source sample.



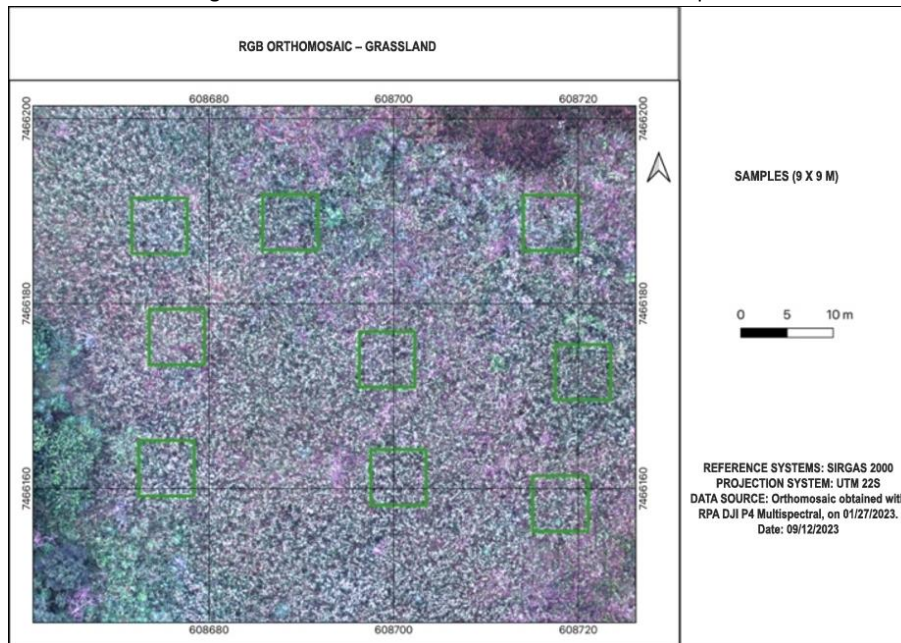
Source: The authors, 2023.

Figure 5 - Orthomosaic in RGB of the Florest sample.



Source: The authors, 2023.

Figure 6 - Orthomosaic in RGB of the Grassland sample.

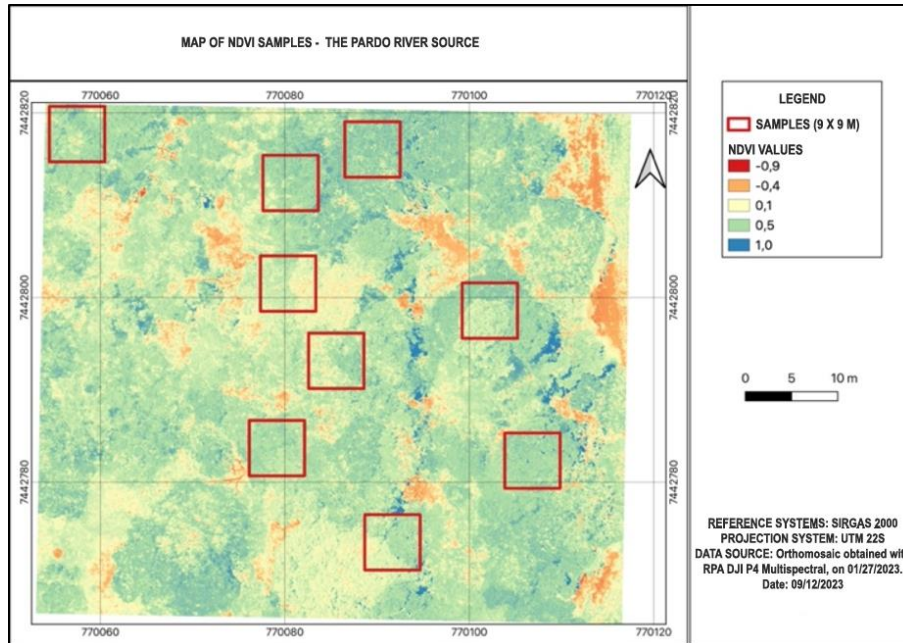


Source: The authors, 2023.

Among the VI maps, it was observed that the NDVI maps (Figures 7, 8 and 9) presented lower rates compared to the SAVI maps. NDVI is an index widely used in monitoring agricultural crops due to its high characteristics regarding plant growth. NDVI values close to 1 represent denser areas of photosynthetically active vegetation, while values close to -1 represent surfaces with less active vegetation (ROSENDO, 2005).

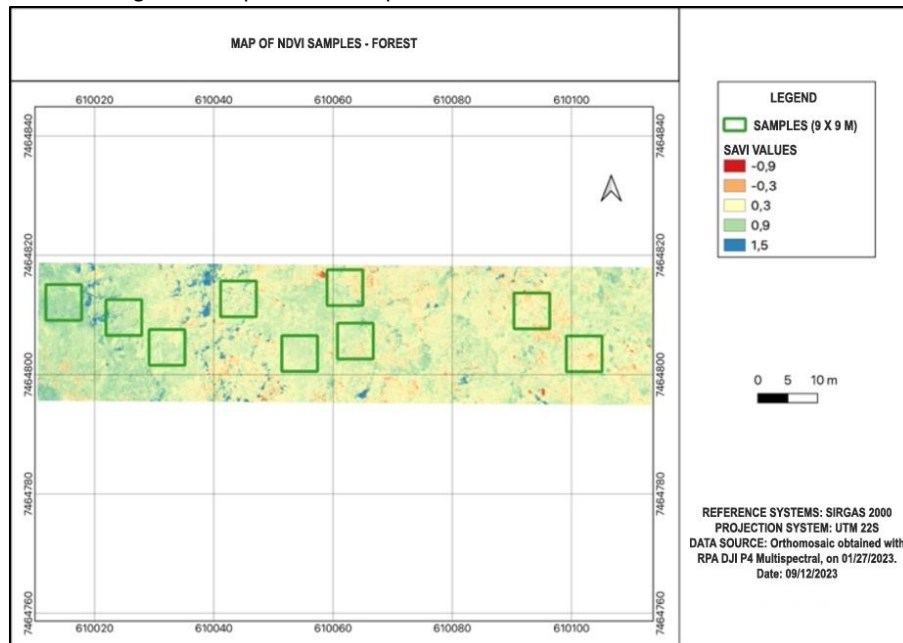


Figure 7 - Map of NDVI samples from the Pardo River Source.



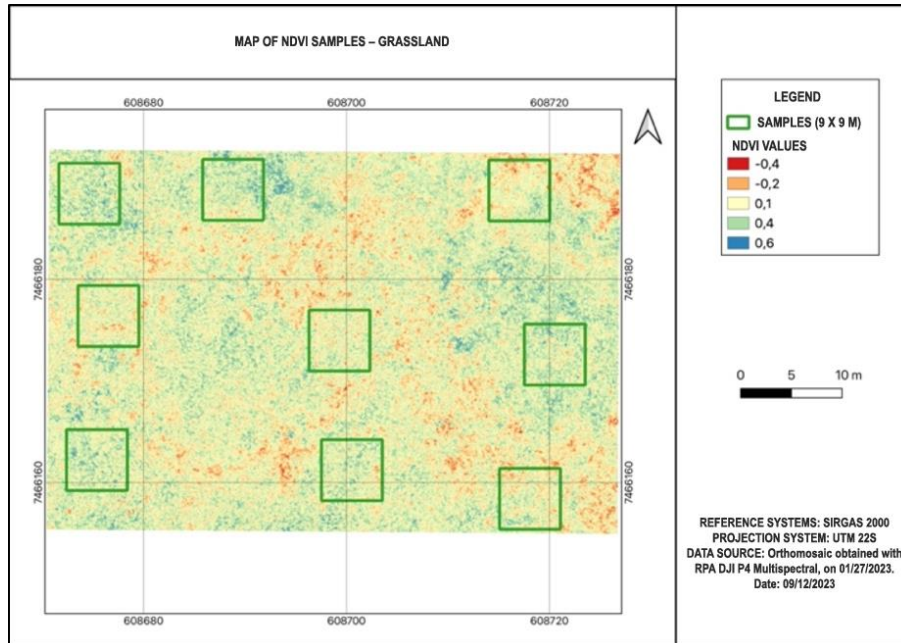
Source: The authors, 2023.

Figure 8 - Map of NDVI samples from an area of the Pardo River Forest.



Source: The authors, 2023.

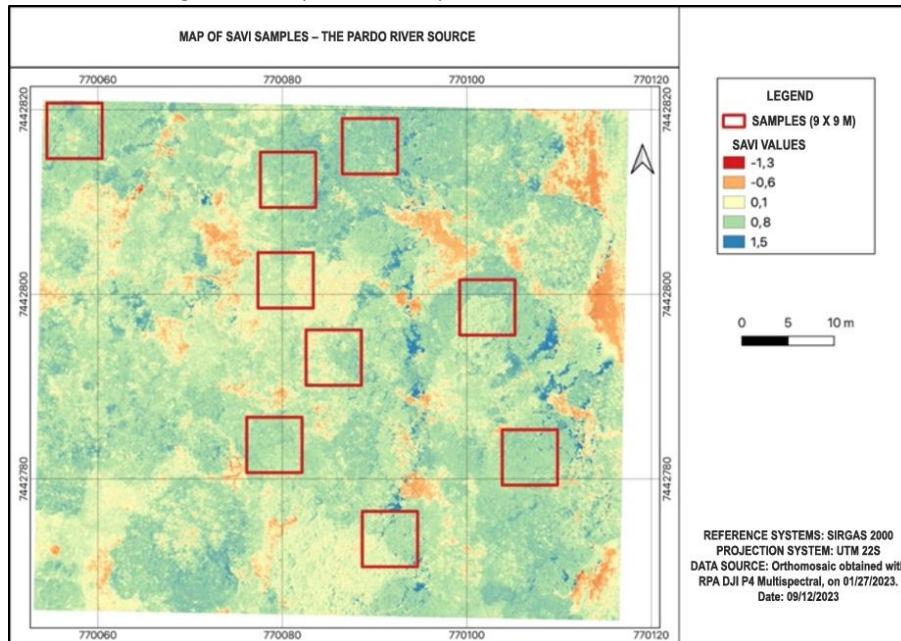
Figure 9 - Map of NDVI samples from an area of the Pardo River Grassland.



Source: The authors, 2023.

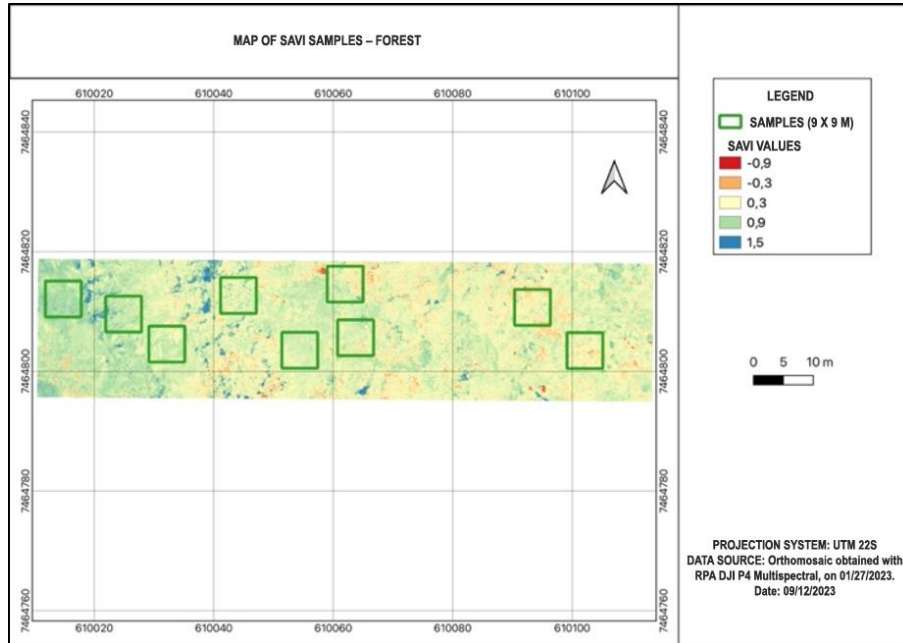
The SAVI maps (Figures 10, 11 and 12) were produced with  $L = 0.5$ , and they presented higher values in relation to the NDVI, proving the reduction of the soil effect (HUETE, 1988; WASHINGTON-ALLEN et al., 2004; MENESES and ALMEIDA, 2012).

Figure 10 - Map of SAVI samples from the Pardo River Source.



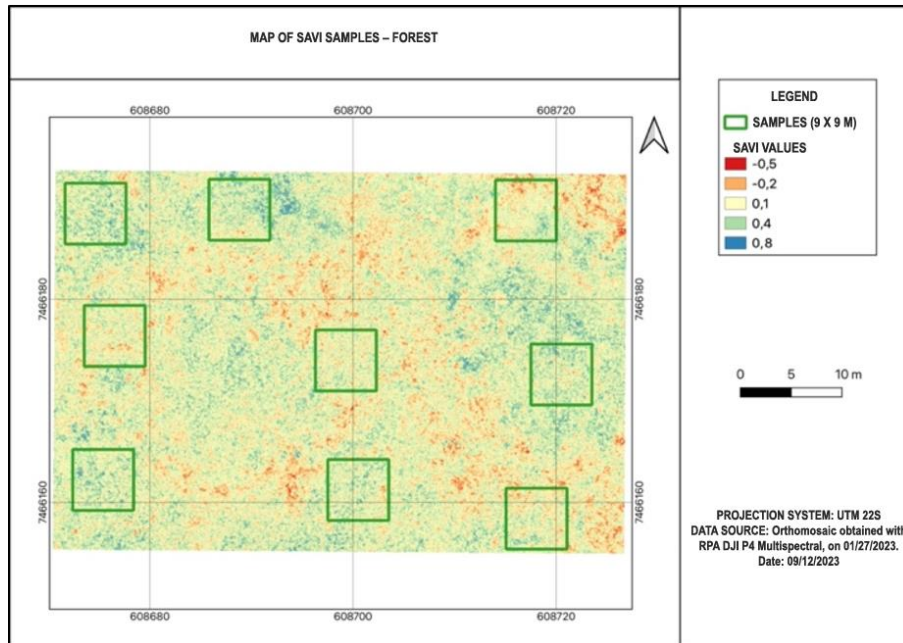
Source: The authors, 2023.

Figure 11 - Map of SAVI samples from an area of the Pardo River Forest.



Source: The authors, 2023.

Figure 12 - Map of SAVI samples from an area of the Pardo River Grassland.



Source: The authors, 2023.

Table 1 presents the average values of the VI and LAI, with the LAI used as a basis for ordering the table, that is, from highest to lowest value.



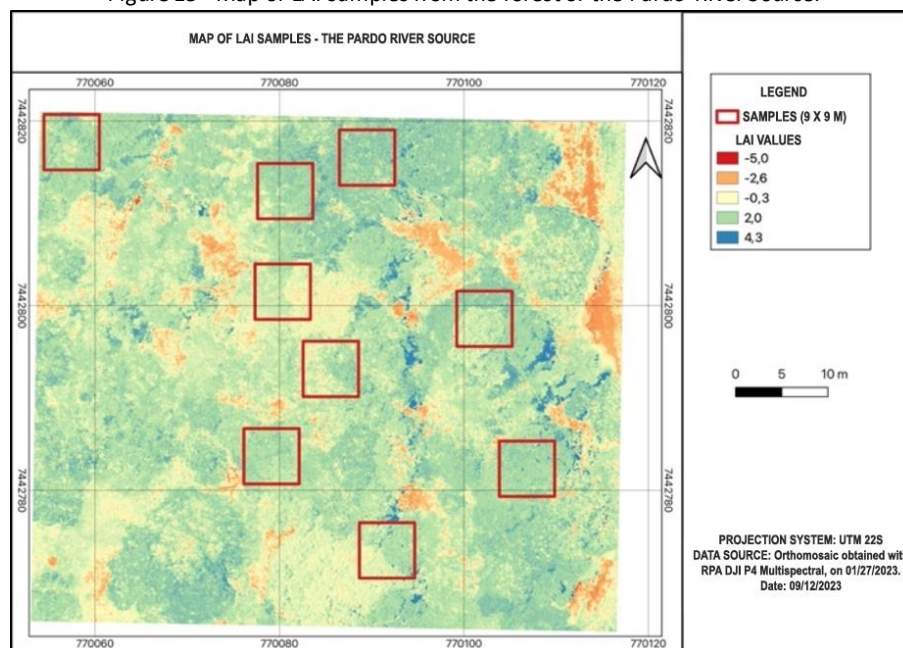
Table 1 - Average values of the VI NDVI, SAVI and LAI samples.

	Source	Grassland	Florest
NDVI	0,455	0,17	0,345
SAVI	0,683	0,213	0,518
LAI	1,715	1,689	-0,148

Source: The authors, 2023.

The highest average NDVI can be observed in the Source class, in the Ortomosaic of Figure 4 and in the VI of Figure 7. The Source class presented the highest NDVI/SAVI index and the highest LAI (Figure 13), indicating that the site is healthy and preserved with mature and leafy species. These results reflect plants with excellent vegetative vigor, with SAVI presenting the highest average with a variation between plants in an excellent state of vegetative activity (JENSEN, 2009; BORATTO, 2013). The higher SAVI average can be explained by the lesser influence of the soil on the VI values (HUETE, 1988).

Figure 13 - Map of LAI samples from the forest of the Pardo River Source.

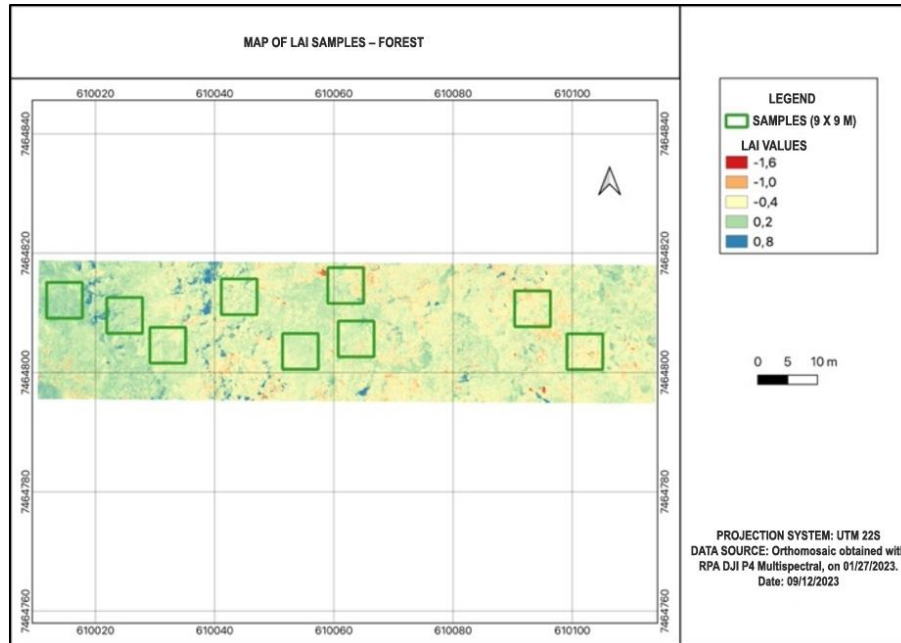


Source: The authors, 2023.

The Forest class presented the second highest average of NDVI/SAVI, which also demonstrates healthy vegetation in full development. However, as can be seen in Table 1, the LAI of the Forest class presented the lowest average in relation to the other samples, which can also be seen in Figure 14. It is observed that this result was influenced by the low density of leafy trees and with a greater incidence of reflectance from the wet and muddy soil due to the abundant rain in the period prior to the aerial survey, as can be seen in the graph in Figure 15, which shows that the month of January reached an accumulated rainfall of 197.5 mm . Another factor that influenced the low LAI value was the presence of leaves with light tones and flowers in several species (Figure 5), resulting in a reduction in chlorophyll and, consequently, the NDVI/SAVI values are lower (HUETE, 1988; BORATTO, 2013; ZHANG, 2014).

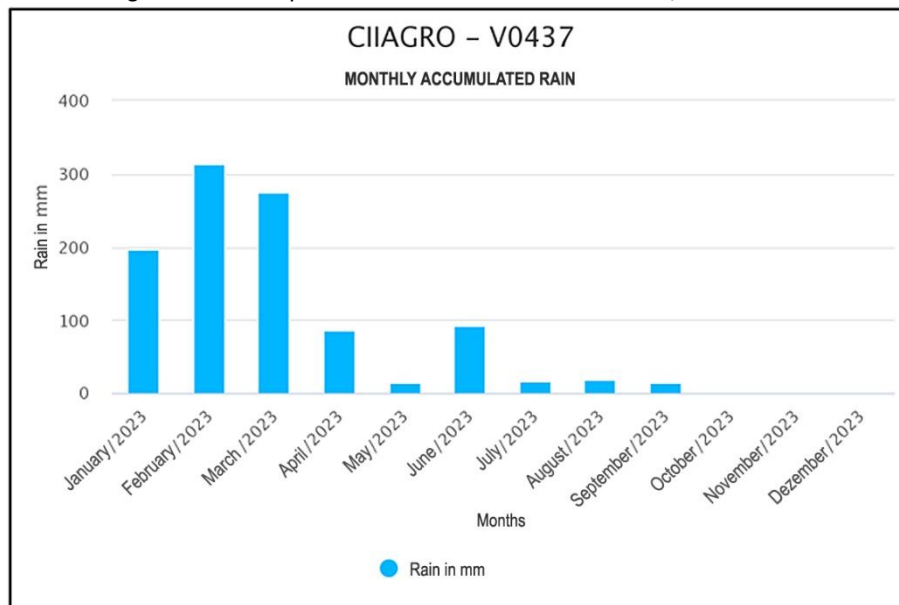


Figure 14 - Map of LAI samples from an area of the Pardo River Forest.



Source: The authors, 2023.

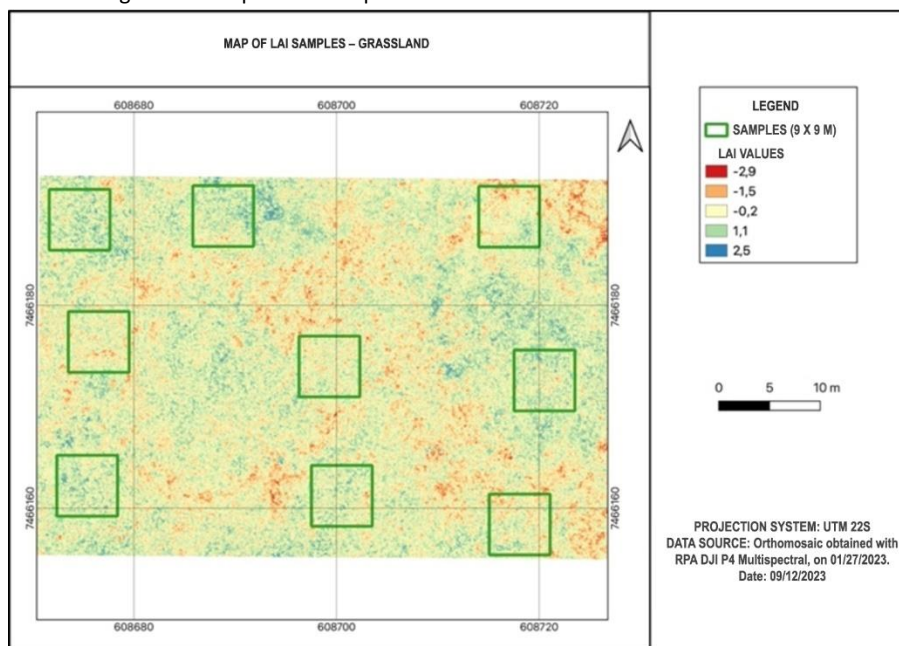
Figure 15 - Monthly accumulated rainfall at station V0437, Ourinhos-SP.



Source: <https://tempo.inmet.gov.br/PrecAcumulada>.

The means of the Grassland class samples presented the lowest NDVI/SAVI values (Table 1), these values can be explained by the moisture present in the soil. However, the LAI was the second highest, being close to the value of the source class (Figure 16). The high LAI can be attributed to a large amount of broadleaf vegetation and abundant biomass in the samples.

Figure 16 - Map of LAI samples from an area of the Pardo River Grassland.



Source: The authors, 2023.

The results presented by the Grassland class are in line with similar studies carried out by Lima (2017), where the characteristics of this vegetation class favored the NDVI/SAVI to obtain Agriculture / Field / Soil typology values.

In addition to the qualitative analyses of the images, statistical analyses were also carried out, where, based on correlation tests, the LAI was identified as the dependent variable of the regression, as it has significant statistical correlations with the independent variables NDVI and SAVI (FIGUEIREDO FILHO and SILVA JUNIOR, 2009). In Table 2 it is observed that the regression analysis of the dependent variable LAI with the independent variables NDVI and SAVI resulted in significant positive relationships for all tested variables.

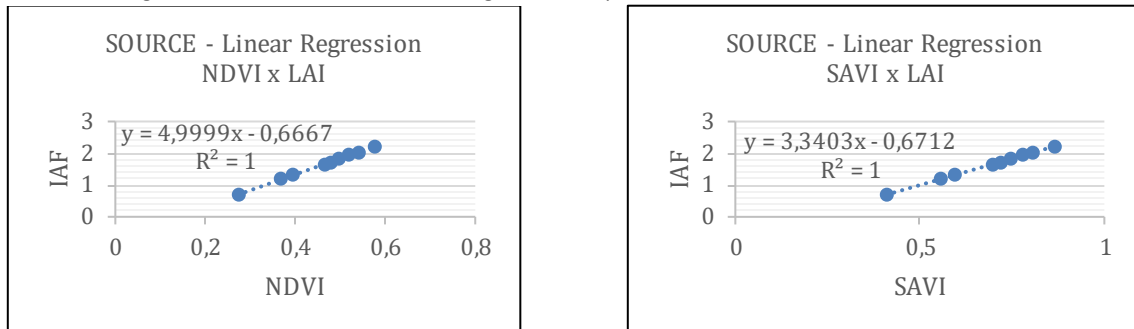
Table 2 - Statistics and coefficient of determination ( $r^2$ ) of the linear regression of VI x LAI.

Dependent variable	Statistics		Independent variable		Vegetation class According to LAI Table 1
	NDVI (valor P)	SAVI (valor P)	NDVI ( $r^2$ )	SAVI ( $r^2$ )	
LAI	4,3423E-34	1,75028E-15	1	0,9999928	Source
LAI	8,96184E-40	7,92465E-17	1	0,999979603	Grassland
LAI	1,82876E-20	1,0253E-18	0,999995093	0,999984494	Forest

Source: The authors, 2023.

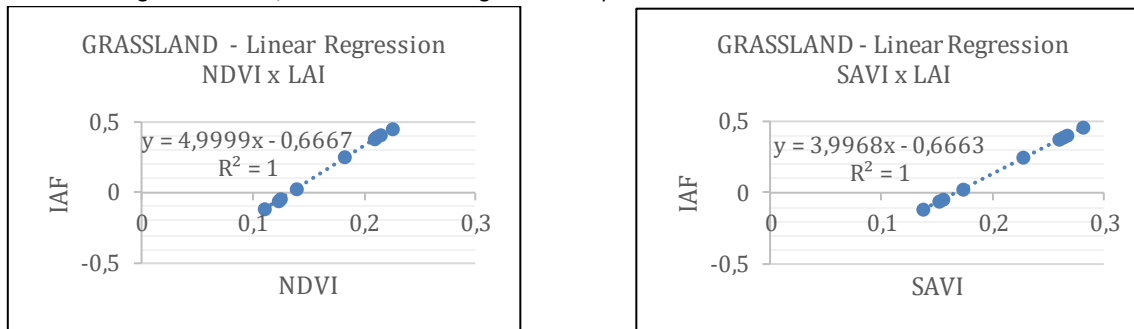
The graphs represented by Figures 17, 18 and 19 show the correlations between NDVI/SAVI x LAI of vegetation classes in the same ordering sequence presented in Table 1 (according to LAI values). Observe the adequate distributions along the straight lines of simple linear regression values.

Figure 17 - NDVI/SAVI x LAI Linear Regression Graphs of the forest of the Pardo River Source.



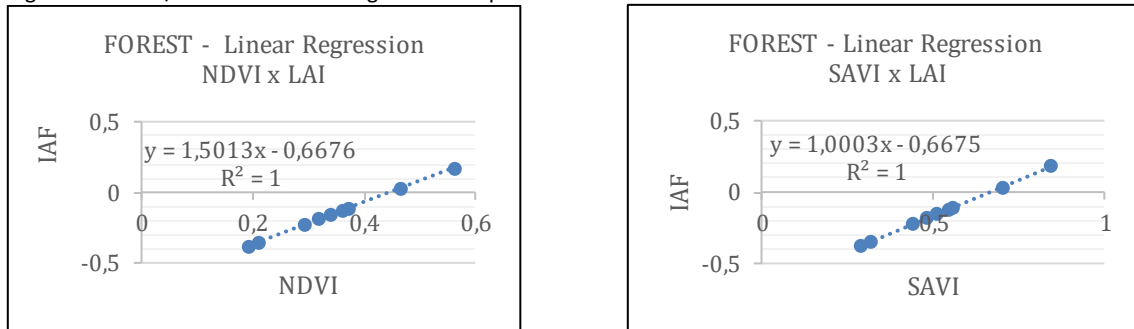
Source: The authors, 2023.

Figure 18 - NDVI/SAVI x LAI Linear Regression Graphs of an area of the Pardo River Grassland.



Source: The authors, 2023.

Figure 19 - NDVI/SAVI x LAI Linear Regression Graphs of an area of the Pardo River Forest.



Source: The authors, 2023.

Analyzing the data from the vegetation class plots, it is possible to verify that in areas where the vegetation is lower and with sparse tree canopies, the soil exerts a greater negative influence on the VI results and consequently on the LAI. This influence can be observed in all maps referring to VI and LAI. The positive regression indicates that the higher the VI SAVI values, the higher the LAI. It is also possible to verify that the higher the LAI, the greater the height of the canopy in the forest, as well as its distribution and overlapping of leaves, which corroborate the decrease in the influence of the soil on the spectral results (SILVA, 2018). The exception to this analysis was the forest class, which presented high SAVI values, but due to the factors

exposed previously, it obtained a LAI below expectations in relation to the other vegetation classes.

## 5 CONCLUSIONS

The results obtained in this study, under the conditions under which the experiment was carried out and with the method applied, allow us to conclude that:

RGB orthoimages acquired by drones have high spatial resolution that enable various analyses of vegetation classes, such as analysis of species identification, distribution and differentiation of vegetation, mapping of clearings or deforestation, among others.

The images obtained from the NDVI showed good results, but in places where there were gaps, spacing and non-uniform distribution of vegetation, the NDVI values were low due to the influence of the moist soil. On the other hand, the images produced with SAVI presented higher values, making it possible to reduce the influence of soil reflectance and humidity on the substrate.

The simple linear regression analysis between the response variable LAI and the predictor variable SAVI showed that the higher the SAVI, the higher the LAI and the higher the height of the vegetation canopy.

NDVI or SAVI surveys carried out during rainy or flowering periods interfere with vegetation indices, due to the increase in humidity in the soil and, in the case of flowers, there is a decrease in chlorophyll in the leaves of the vegetation.

The plots of the source class presented higher density and higher average LAI value, and the higher LAI contributed to reducing the influence of the soil on the spectral response. This characteristic can be observed in all images of the source class, as there is a good development of vegetation, with a homogeneous canopy, favoring a good adjustment of the data.

The images obtained by drones presented very high spatial, temporal and spectral resolution, thus, it is concluded that drones are great platforms for the management and constant monitoring of permanent preservation areas (PPA).

Finally, there is a need for special care when obtaining multispectral images, as these images require appropriate methods to be obtained and depending on the sensor, there is a need for radiometric calibration of the camera.

## Acknowledgements

The authors would like to thank the Water Security Research Group (GPSH) and the Brazilian Center for UAVs for Air Surveys (NUBRAVA) for their support with equipment and facilities and the universities UTFPR-PB and FCTE/UNESP – Ourinhos, for their scientific support.

## REFERENCES

ADAM, Elhadi; MUTANGA, Onisimo; RUGEGE, Denis. Multispectral and hyperspectral remote sensing for identification and mapping of wetland vegetation: a review. **Wetlands Ecology and Management**, Springer Netherlands, v. 18, p. 281-296, dez. 2009.



ALLEN, Richard; TASUMI, Masahiro; TREZZA, Ricardo. **SEBAL Surface Energy Balance Algorithm for Land - Advanced Trainig and User Manual**, Idaho Implementation, v. 1.0, 2002

ALMEIDA, A. Q.; RIBEIRO, A. DELGADO, R. C.; RODY, Y. P.; OLIVEIRA, A. S.; LEITE, F. P. Índice de área foliar de *Eucalyptus* estimado por índices de vegetação utilizando imagens TM – Landsat 5. **Floresta e Ambiente**, v. 22, n. 3, p. 368-376, 2015.

BOON, Marinus Axel; GREENFIELD, Richard; TESHAMICHAEL, Solomon. Unmanned aerial vehicle (UAV) photogrammetry produces accurate high-resolution orthophotos, point clouds and surface models for mapping wetlands. **South African Journal of Geomatics**, v. 5, n. 2. p. 186-200, set. 2016.

BORATTO, I. M. P; GOMIDE, R. L. Aplicação dos índices de vegetação NDVI, SAVI e IAF na caracterização da cobertura vegetativa da região Norte de Minas Gerais. In: SIMPÓSIO BRASILEIRO DE SENSORIAMENTO REMOTO, 16., 2013, Foz do Iguaçu. **Anais eletrônicos [...]** São José dos Campos: INPE, 2013. p.7345-7352. Available at: <<http://www.dsr.inpe.br/sbsr2013/files/p0075.pdf>>. Access on: 01 jul. 2023.

ELIAS, Adão Robson. Uso de tecnologias (Drones) Visando ao Planejamento Conservacionista. In: OROMAR, João Bertol (Org.). **Manual de manejo e conservação do solo e da água para o Estado do Paraná**. 1ª Ed. Curitiba (PR): Editora Cubo, 2019. P. 93-102.

FELIPETTO, H. S. *et al.* UAV application in wheat crop: a bibliometric approach to the literature. **Revista ciência Agrônômica**. V. 54. E20228592, Jan. 2023. DOI: 10.5935/1806-6690.20230025.

FERRAZ, A. S.; SOARES, V. P.; SOARES, C. P. B.; RIBEIRO, C. A. S. A; GLERIANI, J. M. Uso de imagens do satélite IKONOS II para estimar biomassa aérea de um fragmento de floresta estacional semidecidual. In: XVI SIMPÓSIO BRASILEIRO DE SENSORIAMENTO REMOTO - SBSR, 16, 2013, Foz do Iguaçu-PR, **Anais**, Brasil, INPE. 2013. P. 2794-2801.

FIGUEIREDO FILHO, Dalson Britto; SILVA JÚNIOR, José Alexandre. Desvendando mistérios do Coeficiente de Correlação de Pearson (r)\*. **Revista Política Hoje**, v. 18, p. 115-146, 2009.

FONSECA, Jairo Simon; MARTINS, Gilberto de Andrade. **Curso de estatística**. São Paulo-SP, Atlas, 2009.

FUSTINONI, Francesco. **Assessment of capabilities of UAV multispectral imaging for wetland vegetation mapping**. Supervisor: Dr. Giovanna Sona. 2021. 110 f. Master of Science (Dissertação) – School of Civil, Environmental and Land Management Engineering, Politecnico Milano 1863, Milão – Itália, 2021.

GALVÍNCIO, Jocieda Domiciano; MENDES, S. M., MORAIS, Y. C. B., MIRANDA, R. Q., SOUZA, W. M., MOURA, M. S. B. SANTOS, W. Correlação linear entre a precipitação e o Índice de Área Foliar do bioma Caatinga. **Revista Brasileira de Geografia Física**, v. 13, p. 3304-3314, 2020. Available at: <https://doi.org/10.26848/rbgf.v13.07>. Access on: 01 jul. 2023.

HUETE, A. R. Adjusting Vegetation Indices for Soilin fluencies. **Internationl Agrophysics**, v.4, n. 4, p. 367-376, 1988.

HUSSON, Eva; REESE, Heather & ECKE Frauke. Combining spectral data and a DSM from UAS - images for improved classification of non-submerged aquatic vegetation. **Remote Sensing**, v. 9, n. 3, p. 247-262, mar. 2017.

JENSEN, John R. 2009. **Sensoriamento Remoto do Ambiente – Uma perspectiva em recursos terrestres**. São José dos Campos-SP, Parêntese, 2009.

LIMA, Diego Ricardo Medeiros de; DLUGASZ, Fernando Luís; IURK, Mariângela Ceschim; PESK, Vagner Alex. Uso de NDVI e SAVI para caracterização da cobertura da terra e análise temporal em imagens RapidEye. **Revista ESPACIOS**, v. 38, n. 36, p. 7-21, mar. 2017.

MENESES, Paulo Roberto; ALMEIDA, Tati de. **Introdução ao Processamento Digital de Imagens de Sensoriamento Remoto**. Brasília: Universidade de Brasília, 2012.

MIKHAIL, Edward M.; BETHEL, James S.; MCGLONE, Chris. **Introducion to Modern Photogrammetry**. New York: John Wiley & Sons, 2001.

PIROLI, Edson Luís. **Águas e bacias hidrográficas: planejamento, gestão e manejo para enfrentamento das crises hídricas**. São Paulo: Editora Unesp Digital, 2022.

ROSENDO, Jussara dos Santos. **Índices de vegetação e monitoramento do uso do solo e cobertura vegetal na Bacia do Rio Araguari – MG – utilizando dados do sensor MODIS**. Orientador: Roberto Rosa. 2005. 130 p. Dissertação de Mestrado, Programa de Pós-Graduação em Geografia, Universidade Federal de Uberlândia, Uberlândia-MG, 2005.



ROUSE, J. W.; HAAS, R. H.; SCHELL, J. A.; DEERING, D. W. Monitoring vegetation systems in the great plains with ERTS. *In: EARTH RESOURCES TECHNOLOGY SATELLITE-1 SYMPOSIUM*, 3, 1973, Proceedings. Washington, **Anais** [...] Washington: 1973, p. 309-317.

SILVA, Elizabeth Dell'Orto. **Sensoriamento remoto por meio de uma aeronave remotamente pilotada para estudo do manguezal da Baía de Vitória**. Supervisor: Dr<sup>a</sup>. Mônica Maria Pereira Tognella. 2018. 104 f. Tese de Doutorado – Pós-Graduação m Oceanografia Ambiental, Universidade Federal do Espírito Santo, Vitória, Espírito Santo, Brasil, 2018.

WASHINGTON-ALLEN, R. A. W; RAMSEY, R. D; WEST, N. E. Spatiotemporal mapping of the dry season vegetation response of sagebrush steppe. **Community Ecology**, v. 5, n. 1, p. 69-79, JUN. 2004.

ZHANG, Chunhua; KOVACS, John M.; LIU, Yali; FLORES-VERDUGO, Francisco; FLORES-de-Santiago, Francisco. Separating Mangrove Species and Conditions Using Laboratory Hyperspectral Data: A Case Study of a Degraded Mangrove Forest of the Mexican Pacific. **Remote Sensing**, Canada, v. 6, n. 12, p. 11673-11688, nov. 2014.

ZWEIG, Christa L.; BURGESS, Matthew A.; FRANKLIN, Percival H.; & KITCHENS, Wiley M. Use of unmanned aircraft systems to delineate fine-scale wetland vegetation communities. **Wetlands**, USA, v. 35, n. 2, p. 303-309, fev. 2015.